MUSCULOSKELETAL MODEL FOR THE RAT HIND LIMB

U. Simon[a,b], T. Wehner[a], I. Cosgun[a], T. Henzler[a], L. Claes[a,b], and U. Wolfram[a]

a) Institute of Orthopaedic Research and Biomechanics, University of Ulm, Germany, www.biomechanics.de
b) Ulm Center for Scientific Computing, University of Ulm, Germany, www.uzwr.de

1 INTRODUCTION

In clinical research the rat is used for experimental testing of new implants, implant materials and fracture healing methods. The advantage of the rat as an experimental animal in comparison to bigger animals, i.e. dog or sheep, is the availability of a great amount of immuno-biological methods. Nevertheless, economic as well as ethical concerns restrict the number of possible experiments. However, for a proper design and evaluation of those experiments the knowledge of the musculoskeletal loads is essential. Besides experimental testing, numerical models have been used to simulate the fracture healing process (e.g. [1] – [3]). The quality of those simulations is directly dependent on the used input data, i.e. the bone internal loads. To provide these input data and to prove the numerical models a vast serial of animal experiments would be necessary. However, it is very problematic to determine the internal loads since they are depending on the muscle forces which are very problematic to be measured during gait. Therefore, an inverse-dynamic simulation of the musculoskeletal system of the rat is performed to determine these muscle forces.

2 METHODS

To determine the muscle forces in an inverse-dynamic simulation it was necessary to define an anatomical model of the hind limb of the rat. We conceived the hind limb as a system of rigid bodies. Figure 1 and Table 1 are depicting the defined rigid bodies as well as the introduced joints. The mass parameters for the rigid bodies were gained from high resolution (spatial resolution of 160µm) computer tomography images of a hind limb of a rat.

In addition to the bone mass the muscle mass was already taken into account through the definition of the rigid bodies as well. The line of action of each muscle was modeled as a vector chain having up to eight deviating points. To calculate tensile stresses a physiological cross sectional area (PCSA) for each muscle needs to be determined. The PCSA was defined according to [4].

The masses of the muscles were taken from literature [5]. In cases where we were not able to find a value for the muscle mass, we estimated it by comparing it to known muscles using anatomy atlases. After all, 35 of the 41 muscles of the hind limb were modeled giving 81 vector chains. This number seems to be quite high but is simply due to the fact that multiheaded muscles were represented by a sufficient amount of separated vector chains.

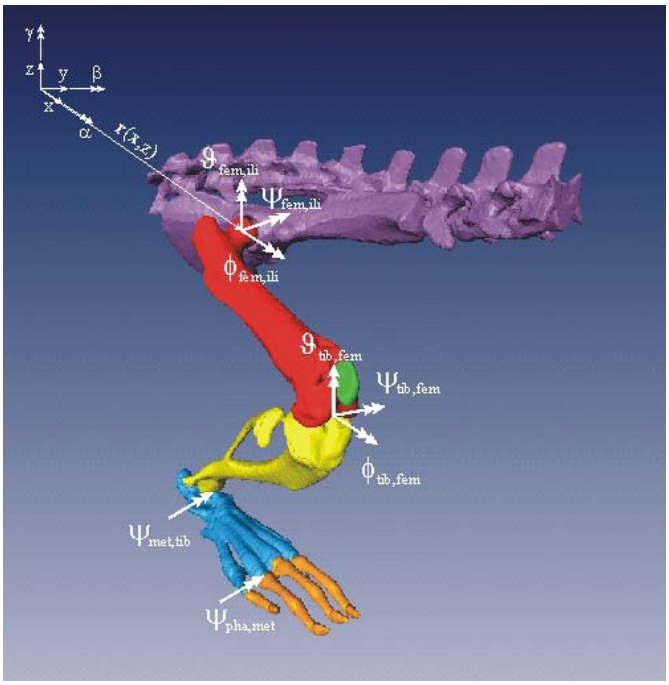

Figure 1: Defined rigid bodies (left) and introduced joints (right).

Table 1: Rigid bodies and introduced coordinates used in the gait analysis as depicted in Figure 1.

Abbr.	Connected Bodies	Respective Joint	Given DOFs
pha,met	Phalanges-Metatarsus	phalangeal-metatarsal joint	1 revolution
met,tib	Metatarsus-Tibia	talus and ankle joint	1 revolution
tib,fem	Tibia-Femur	knee joint	3 revolutions
fem,ili	Femur-Pelvis	hip joint	3 revolutions
ili,global	Ilium-Global system	driver joint	3 revolutions 3 translations

	Variable	Meaning
Translatory	x	Translation in x-direction of the acetabulum
	z	Translation in z-direction of the acetabulum
Rotatory	$\psi_{pha,met}$	Rotation of the phalanges with respect to the metatarsals about the metatarso-phalangeal-joint
	$\psi_{met,tib}$	Rotation of the metatarsals with respect to the tibia about the ankle joint
	$\psi_{tib,fem}$	Rotation of the tibia with respect to the femur about the knee joint
	$\psi_{fem,ili}$	Rotation of the femur with respect to the ilium about the acetabulum
	$\psi_{ili,global}$	Rotation of the ilium with respect to a horizontal line through the acetabulum about the acetabulum

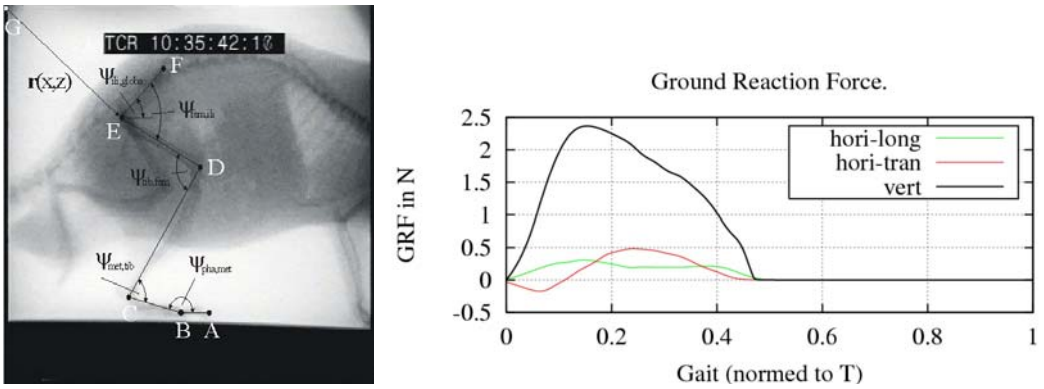

Figure 2: Exemplary gait analysis for one time point (left) and the graph of the ground reaction forces (right). Stance phase lies within the first half of the recorded cycle and swing phase in the last half.

The gait analysis was performed on dynamic radiography images from walking as depicted in Figure 2. At time points we measured the relative joint angles. Stride time lasted for roughly 500 ms and stride length was approximately 117 mm. Ground reaction forces measured on rats while walking (Figure 2) were taken from the literature as well [6]. After the ground reaction forces are applied the model can be solved.

We used a house own developed inverse-dynamics software [7] as well as the Anybody software (www.anybodytech.com) to solve for the unknown muscle forces. The hind limb of the rat is established with a degree of freedom of 15. At the same time 81 unknown muscle forces need to be found.

Figure 3: Complete musculoskeletal model of the rat hind limb in the software Anybody (www.anybodytech.com).

This load distribution problem was solved by applying an optimization criterion, which tries to minimize the sum of the squared muscle stresses.

$$\begin{aligned} &\text{minimize} && G(\sigma_{Mus}) = \sum_{i}^{n_M} \sigma_{Mus,i}^2 \\ &\text{subject to} && \begin{bmatrix} \mathbf{C} & \mathbf{C_M} \end{bmatrix} \begin{bmatrix} \lambda \\ \mathbf{f}_{Mus} \end{bmatrix} = \begin{bmatrix} \mathbf{f_{a,i}} - \mathbf{M\ddot{r}} \\ \mathbf{m'_{a,i}} - \Theta\dot{\omega}' + \tilde{\omega}'\Theta\omega' \end{bmatrix} \\ &\text{and} && \mathbf{bl} \leq \sigma_{Mus} \leq \mathbf{bu} \end{aligned}$$

4 RESULTS AND DISCUSSION

The model was solved for the muscle forces and the hip contact forces. Both software packages showed practically identical results. The hip contact forces showed the typical two peak behavior for quadrupeds. The peak hip contact force was found to be about four times the body weight of the animal (Figure 4). All calculated muscle forces lay below two times the body weight of the animal. The muscles forces of selected muscles did fit quite well to EMG activation patterns found in the literature [8] as Figure 5 suggest.

However, there were muscle forces which showed unphysiological peaks or which do not fit to EMG activation patterns very well. In the first case this can

be due to the applied optimization criterion. The latter happened to occur in muscles which can not serve their actual degree of freedom in our simplified model, e.g. musculus hallucis longus. Since we were just able to gain the gait data from two dimensional images (see Figure 2), we could not obtain enough information for every muscle especially in the lower limb. This is as well the reason why we defined revolute joints between metatarsals and phalanges.

The hip contact forces seemed to be quite high in comparison to other quadrupeds, here the sheep (Figure 4) with up to two times the body weight of the animal. However, the rat is characterized by a lot more muscle mass than the hind limb of the sheep compared to the bone mass, which indicate that higher relative loads might be reasonable.

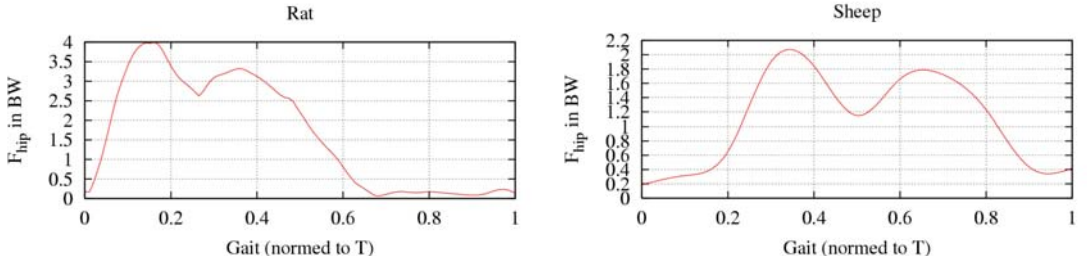

Figure 4: Absolute amount of hip contact forces in BW for the rat (left) and in comparison for the sheep (right). Stance phase for left diagram lies within the first half of the plot but in the middle of the plot (roughly from about 0.3 to 0.8) for the right diagram.

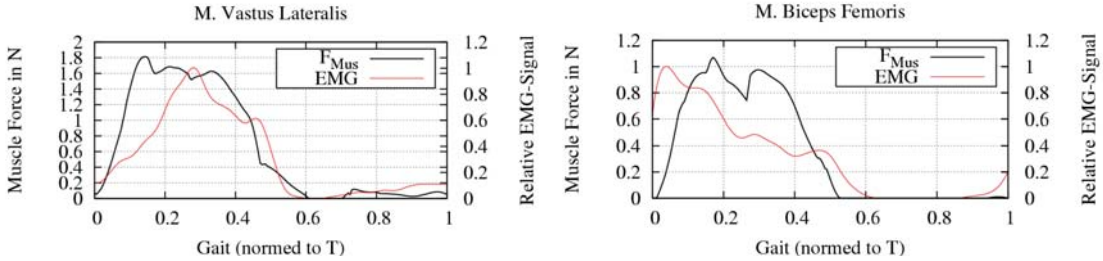

Figure 5: Results. Forces for musculus vastus lateralis (left) and musculus biceps femoris (right) over gait cycle.

Furthermore, we checked whether the contact stress in the hip joint exceeds a critical value for cartilage, which was not the case.
From these feasibility factors we conclude that the calculated hip contact forces are possible.
On the other hand if one compares the rat to bigger animals, e.g. an elephant, one will find that the bigger animal stands on almost straight, vertical oriented legs. This is not the case in the rat's gait where the femur is quite inclined with respect to the vertical direction. Hence, the rat needs to equilibrate this flexed position while standing and walking with increased muscle forces (the extensors). This could as well explain the higher hip contact forces compared to sheep.

5 REFERENCES

[1] Doblare, M.; Garcia, J. M.: On the modelling bone tissue fracture and healing of the

bone tissue. Acta Cient Venez. 54 (1): 58 – 75, 2003.
[2] Lacroix, D.; Prendergast, P.: A mechano-regulation model for tissue differentiation during fracture healing: analysis of gap size and loading. J. Biomech 35: 1163 – 1171, 2002.
[3] Simon, U.; et. al.: Simulation of tissue development and vascularization in the callus healing process. In Proc. of 49th Annual Meeting of the Orthopaedic Research Society (ORS). New Orleans. Paper Nr. 0299, 2003.
[4] Heerkens, Y. F.; et. al.: Mechanical properties of passive rat muscle during sinusoidal stretching. Pflüges Arch. 409: 438 – 447, 1987.
[5] Armstrong, R. B.; Phelps, R. O.: Muscle fiber type composition of the rat hindlimb. Am. J. Anat. 171: 259 – 272, 1984.
[6] Muir, G. D.; Whisaw, Q. I.: Ground reaction forces in locomoting hemi-parkinsonian rats. Exp. Brain Res. 126: 307 – 314, 1999.
[7] Forster, E.; et. al.: Extension of a state-of-the-art optimization criterion to predict cocontraction. J. Biomechanics 37: 577 – 581, 2004.
[8] Nicolopoulos-Stournaras, S.: Hindlimb muscle activity during locomotion in the rat. J. Zool. 203: 427 – 440, 1984.